

## Universal Kardar-Parisi-Zhang Dynamics in Integrable Quantum Systems

Bingtian Ye<sup>1,2,\*</sup>, Francisco Machado<sup>1,3,\*</sup>, Jack Kemp<sup>1,\*</sup>, Ross B. Hutson<sup>1,4,5</sup>, and Norman Y. Yao<sup>1,2,3</sup>

<sup>1</sup>Department of Physics, University of California, Berkeley, California 94720, USA

<sup>2</sup>Department of Physics, Harvard University, Cambridge, Massachusetts 02138, USA

<sup>3</sup>Materials Sciences Division, Lawrence Berkeley National Laboratory, Berkeley, California 94720, USA

<sup>4</sup>JILA, National Institute of Standards and Technology, Boulder, Colorado 80309, USA

<sup>5</sup>Department of Physics, University of Colorado, Boulder, Colorado 80309, USA



(Received 24 May 2022; revised 8 August 2022; accepted 23 September 2022; published 30 November 2022)

Although the Bethe ansatz solution of the spin-1/2 Heisenberg model dates back nearly a century, the anomalous nature of its high-temperature transport dynamics has only recently been uncovered. Indeed, numerical and experimental observations have demonstrated that spin transport in this paradigmatic model falls into the Kardar-Parisi-Zhang (KPZ) universality class. This has inspired the significantly stronger conjecture that KPZ dynamics, in fact, occur in *all* integrable spin chains with non-Abelian symmetry. Here, we provide extensive numerical evidence affirming this conjecture. Moreover, we observe that KPZ transport is even more generic, arising in both supersymmetric and periodically driven models. Motivated by recent advances in the realization of  $SU(N)$ -symmetric spin models in alkaline-earth-based optical lattice experiments, we propose and analyze a protocol to directly investigate the KPZ scaling function in such systems.

DOI: 10.1103/PhysRevLett.129.230602

First proposed in the context of surface growth [1], the Kardar-Parisi-Zhang (KPZ) equation has become central to our understanding of many stochastic processes [2–4]. While the central limit theorem ensures that the late-time physics of linear stochastic processes is typically Gaussian, the KPZ equation evades this fate. Instead, it represents a distinct universality class which emerges in myriad dynamical phenomena, ranging from directed polymers and traffic models to kinetic roughening [5–14].

The characterization of dynamical universality classes requires one to specify both the scaling exponents and functions of the theory. This is perhaps most familiar in the context of Brownian motion, where the diffusive late-time behavior follows a Gaussian scaling function; the width of the corresponding distribution grows as  $\sim t^{1/z}$ , where  $z = 2$  is the dynamical scaling exponent. By contrast, the scaling functions for the KPZ universality class are significantly more complex and their exact functional form represents a relatively recent mathematical achievement [8,15–19]. The associated dynamical scaling exponent is neither diffusive nor ballistic ( $z = 1$ ), but rather superdiffusive with  $z = 3/2$ .

Typically, KPZ behavior is expected in nonlinear, out-of-equilibrium *classical* systems subject to external noise; in this context, its observation is extremely robust and does not require any fine-tuning or the presence of a particular symmetry. To this end, the numerical and experimental observation of KPZ universality in a one-dimensional *quantum* spin chain (i.e., the spin-1/2 Heisenberg model), fine-tuned for *both* integrability and  $SU(2)$  symmetry, has attracted widespread attention [20–29]. Interestingly, this

observation is at odds with conventional expectations for spin chain transport, which predict diffusion [30–33]. This naturally motivates the following question: Is the Heisenberg chain an isolated exception, or the first example of a broader group of quantum models in the KPZ universality class?

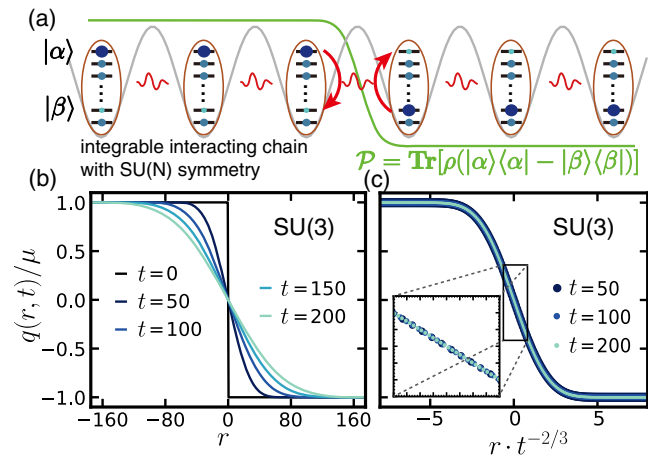


FIG. 1. (a) Schematic depicting a one-dimensional chain of alkaline-earth atoms (each with  $N$  levels) trapped in an optical lattice and interacting via nearest-neighbor superexchange. The equilibration of an initial domain-wall-like imbalance encodes the underlying KPZ dynamics. (b) Domain-wall dynamics as a function of time for an  $SU(3)$ -symmetric, integrable spin chain. (c) The polarization profiles at different times collapse upon rescaling with  $t^{-1/2}$ . The dynamical exponent,  $z = 3/2$ , indicates superdiffusion and is consistent with KPZ transport.

Seminal recent work has made elegant progress on this question by proving that *all* integrable spin chains with a non-Abelian symmetry exhibit superdiffusive transport with  $z = 3/2$  (Fig. 1) [25,28,29]. However, a single scaling exponent does not uniquely specify the universality class and no analysis has been able to determine the nature of the corresponding scaling functions.

In this Letter, we present an extensive numerical investigation that supports the following stronger conjecture—the dynamics of all integrable spin chains with a non-Abelian symmetry belong to the KPZ universality class [28,29]. Leveraging a novel tensor-network-based technique dubbed density matrix truncation (DMT) [34,35], we demonstrate that the spin dynamics of such models are precisely *captured by the KPZ scaling function* (Fig. 3). Intriguingly, our numerical observations suggest that the conjecture holds not only for static systems, but also for periodically driven (Floquet) systems [23,36], as well as supersymmetric models.

By applying perturbations to break either the non-Abelian symmetry or the integrability, we characterize the approach to superdiffusive transport from regimes where there is analytical control on the dynamics. We reproduce these analytical results with unprecedented accuracy, both verifying and benchmarking our numerics, as well as providing independent evidence for the purported microscopic mechanism underlying superdiffusion [22,28,29,37]. Finally, we propose an experimental implementation—based upon alkaline-earth atoms in optical lattices—capable of investigating KPZ transport in a variety of  $SU(N)$ -symmetric, integrable models.

In this Letter, we study the universality classes describing the infinite-temperature dynamics for a variety of one-dimensional quantum spin chains. We will focus on the dynamics of a locally conserved charge  $\hat{Q} = \sum_r \hat{q}_r$ , typically spin. If the system is characterized by a dynamical universality class, at late times the correlation function must collapse under an appropriate rescaling of space and time:

$$\langle \hat{q}_r(t) \hat{q}_0(0) \rangle_{T=\infty} \propto t^{-1/z} f\left(\frac{r}{t^{1/z}}\right). \quad (1)$$

This collapse defines the dynamical scaling exponent  $z$  and the scaling function  $f(\xi)$ , which together determine the universality class.

*Probing transport dynamics.*—Let us begin by exploring the dynamical exponent. While  $z$  can in principle be extracted from the behavior of  $\langle \hat{q}_r(t) \hat{q}_0(0) \rangle_{T=\infty}$ , a simpler and more robust numerical setup is to consider the dynamics of a domain wall. More specifically, we perturb an infinite-temperature density matrix with a weak domain-wall-like imbalance in the charge density [Fig. 1(a)] [38]:

$$\rho(t=0) \propto (1 + \mu \hat{q})^{\otimes L/2} \otimes (1 - \mu \hat{q})^{\otimes L/2}, \quad (2)$$

where  $\mu$  determines the strength of the perturbation and  $L$  is the length of the chain.

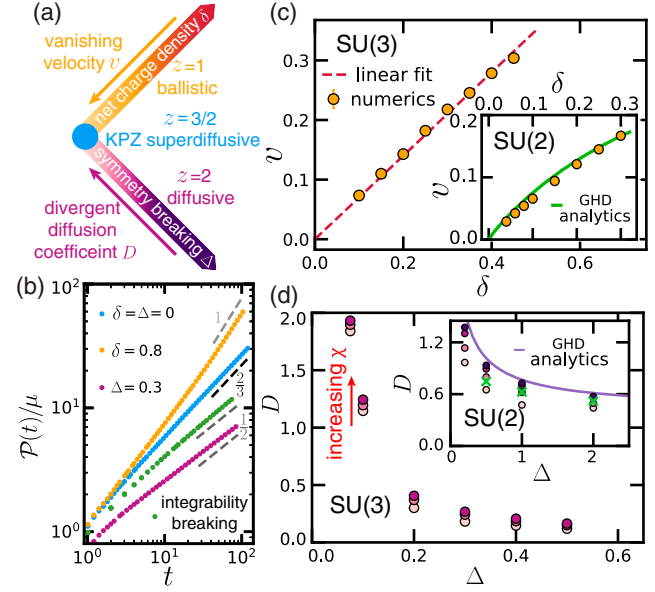


FIG. 2. (a) Conjectured landscape of KPZ transport in integrable, non-Abelian-symmetric models (blue dot). The non-Abelian symmetry can be broken in two distinct ways, either by adding a finite charge density to the initial state (orange line) or by perturbing the underlying Hamiltonian (purple line). (b) The total polarization transferred across the domain wall,  $\mathcal{P}(t)$ , directly determines the dynamical exponent. For the integrable  $SU(3)$  model,  $z = 3/2$ ; when either the integrability or the symmetry is broken in the Hamiltonian,  $z = 2$  [49]; when the initial state has nonzero charge density,  $z = 1$ . Note that the curve for the integrability breaking case (green) is shifted down for clarity. (c) Depicts the charge transport velocity  $v$  as a function of charge density  $\delta$  for both the  $SU(3)$  model and the  $SU(2)$  model (inset) [53]. (d) The diffusion coefficient  $D$  diverges as the Izergin-Korepin and XXZ (inset) integrable models approach the  $SU(3)$  and  $SU(2)$  (inset) symmetric points. The DMT bond dimension  $\chi$  is chosen to be  $\{64, 128, 256\}$  and  $\{64, 128, 256, 512\}$  for the  $SU(3)$  and  $SU(2)$  cases, respectively. Green crosses in the inset mark previous numerical results obtained from tDMRG simulations with bond dimension  $\chi \sim 2000$  [54].

As the system equilibrates, charge crosses the domain wall—the precise details of how this occurs reveals properties of the dynamical universality class [Fig. 1(b)]. In particular, we focus on the spatial profile of the charge density  $q(r, t) = \langle \hat{q}_r(t) \rangle$  (hereafter, denoted as polarization), as a function of time  $t$  and displacement  $r$  from the domain wall. A natural measure of transport is the total polarization transferred across the domain wall,  $\mathcal{P}(t) = \sum_{r=1}^{L/2} [\mu - q(r, t)]$ , which provides a robust way to determine  $z$ :  $\mathcal{P}(t) \propto t^{1/z}$ .

To implement the domain-wall dynamics, we represent  $\rho$  using a matrix product density operator and compute its evolution via DMT [34,35]. The truncation procedure in DMT is specifically designed to preserve local operators, such as the energy density, polarization, and their currents; this choice makes DMT particularly amenable for

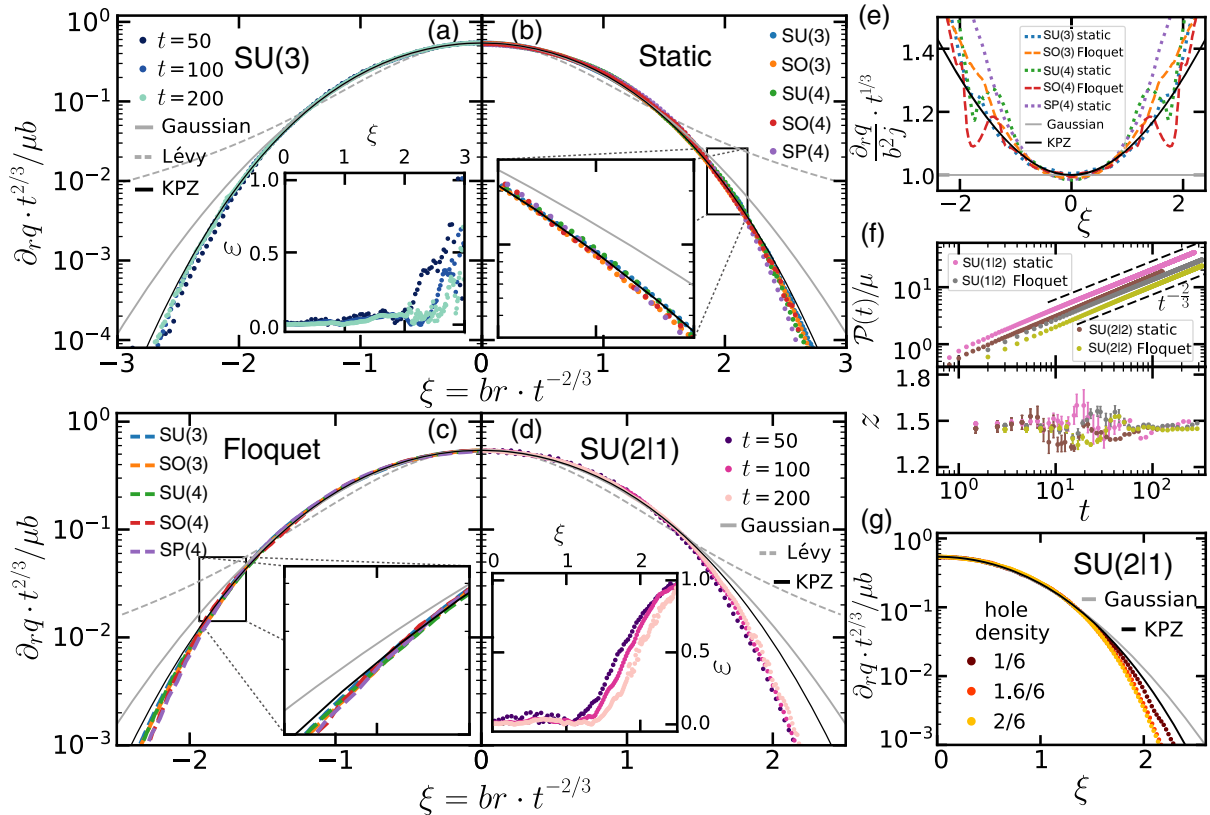


FIG. 3. (a)–(d) The KPZ scaling function emerges from a wide variety of integrable dynamics: static, non-Abelian-symmetric models, their Floquet counterparts, and supersymmetric models. (a)[(d)] At late times, the rescaled polarization profiles of the SU(3)[SU(2|1)] model differ from both the Gaussian and Lévy-flight expectations, but exhibit excellent agreement with the KPZ scaling function. Insets of (a)[(d)]: relative difference with respect to the KPZ scaling function. We note that the agreement extends to longer length scales as time is increased. (b)[(c)] Late-time, rescaled polarization profiles of static [Floquet] integrable models with different non-Abelian symmetries. For all symmetries explored, the dynamics exhibit excellent agreement with the KPZ scaling function. Insets of (b)[(c)]: zoom-in of the polarization profiles. The system sizes in the numerical simulation are chosen as:  $L = 600$  for all static models,  $L = 1200$  for Floquet SU(3) and SO(3) models, and  $L = 800$  for other Floquet models. (e) For all models considered, the ratio between the polarization gradient and the current is inhomogeneous, in stark contrast with the expectation for any linear transport equation. The observed curvature is instead in agreement with KPZ transport. (f) In integrable supersymmetric models, the total charge transferred across the domain wall (upper panel) and the extracted dynamical exponent  $z$  (lower panel) are consistent with superdiffusion. (g) Polarization gradients in an integrable SU(2|1) model with varying hole density. At the same evolution time, systems with a smaller hole density are closer to the KPZ expectation.

probing the universality class of many-body transport dynamics [39].

Although we will explore a wide variety of integrable models (Fig. 3), let us begin by focusing our discussions on the SU(3)-symmetric, spin-1 chain [45–47]:

$$H_{\text{SU}(3)} = \sum_i \hat{\vec{S}}_i \cdot \hat{\vec{S}}_{i+1} + (\hat{\vec{S}}_i \cdot \hat{\vec{S}}_{i+1})^2, \quad (3)$$

where  $\hat{\vec{S}}_i$  is the vector of spin-1 operators acting on site  $i$ . Figure 1(b) depicts the melting of the domain wall as a function of time, starting from the initial state,  $\rho(t=0)$  with  $\hat{q} = \hat{S}^z$  [Eq. (2)]. The corresponding polarization transfer,  $\mathcal{P}(t)$ , exhibits a power law  $\sim t^{2/3}$  [blue line, Fig. 2(b)], consistent with the expected  $z = 3/2$  exponent [48]. This exponent can be independently

confirmed via a scaling collapse of the polarization profile [Fig. 1(c)].

In order to tune the system away from superdiffusion, one can perturb the spin chain by either breaking the non-Abelian symmetry of the underlying equilibrium initial state [28,29] or the symmetry of the Hamiltonian. To study the former, we initialize the system in  $\rho(t=0)$  and add a uniform magnetization  $\delta$  (along the  $\hat{z}$  axis) on each site. The polarization transfer exhibits markedly distinct dynamics with a ballistic exponent,  $z = 1$  [orange line, Fig. 2(b)]. Analytically, for weak magnetizations, the velocity of this ballistic transport is expected to scale linearly with  $\delta$ ; this is indeed borne out by the data [Fig. 2(c)] [22,55]. For the spin-1/2 Heisenberg model, an even stronger statement can be made—the velocity extracted from DMT quantitatively agrees with analytic calculations [via generalized

hydrodynamics (GHD)] even in the nonlinear regime [inset, Fig. 2(c)] [22,37].

Next, we break the symmetry of  $H_{\text{SU}(3)}$  down to U(1) by considering the so-called Izergin-Korepin family of integrable spin-1 models [56–67]. We parametrize the symmetry-breaking strength by  $\Delta$ , such that when  $\Delta = 0$ , we recover  $H_{\text{SU}(3)}$ . For finite values of  $\Delta$ , we observe diffusive transport with the polarization transfer scaling as  $\mathcal{P}(t) \sim t^{1/2}$  [purple line, Fig. 2(b)]. In addition, the extracted diffusion coefficient,  $D$ , diverges as  $\Delta \rightarrow 0$ , consistent with the approach to superdiffusion [Fig. 2(d)]. The analogous numerical experiment in the Heisenberg model, where  $\Delta$  controls the anisotropy of the XXZ model in the easy-axis regime, again quantitatively agrees with analytic calculations.

A few remarks are in order. First, the agreement between DMT numerics and GHD analytics (which have different underlying assumptions) serves a dual benchmarking role; in particular, it highlights DMT’s ability to faithfully characterize late-time transport dynamics and GHD’s ability to quantitatively compute transport coefficients in integrable models [37,54]. Second, in addition to breaking the non-Abelian symmetry of the Hamiltonian, one can also probe the effect of integrability breaking. To this end, we perturb  $H_{\text{SU}(3)}$  using SU(3)-symmetry-respecting, but integrability-breaking next-nearest-neighbor interactions. As expected for generic non-integrable models,  $\mathcal{P}(t) \sim t^{1/2}$ , consistent with diffusive transport [green line, Fig. 2(b)] [50–52].

*Probing KPZ dynamics.*—While our numerical observation of a  $z = 3/2$  exponent in  $H_{\text{SU}(3)}$  clearly establishes the presence of superdiffusion, it does not determine the system’s dynamical universality class. Indeed, such an exponent can also arise in long-range interacting systems exhibiting Lévy flights, as well as rescaled diffusion [20,23,24,68–70].

To this end, we now investigate the universal scaling function. In particular, using our domain-wall dynamics, we can compute the charge correlation function from the spatial gradient of the polarization profile [23]:

$$\langle \hat{q}_r(t) \hat{q}_0(0) \rangle_{T=\infty} = \lim_{\mu \rightarrow 0} \frac{\partial_r q(r, t)}{2\mu} = \frac{b}{t^{2/3}} f\left(\frac{br}{t^{2/3}}\right), \quad (4)$$

where  $b$  is a system-dependent parameter [71].

As depicted in Fig. 3(a),  $\partial_r q(r, t)$  indeed collapses under the rescaling,  $f(\xi = brt^{-2/3})$ . For Lévy flights, one expects power-law tails (gray dashed line), which are manifestly inconsistent with the data. However, the difference between rescaled diffusion and KPZ is more subtle: for the former,  $f(\xi)$  is Gaussian, while for KPZ,  $f(\xi)$  exhibits faster decaying tails  $\sim \exp(-0.295|\xi|^3)$  [16–18]. The data quantitatively agree with the KPZ prediction: The longer the evolution time, the closer  $\partial_r q(r, t)$  is to the KPZ scaling function [highlighted by the relative error, Fig. 3(a) inset]. This agreement allows us to directly extract  $b = 0.460 \pm 0.001$ , which reflects the ratio between the diffusive smoothing, and the nonlinear growth and noise in the

KPZ equation. We emphasize that these observations apply to *any* conserved charges generated by the non-Abelian symmetry [39].

A complementary way to distinguish between rescaled diffusion and KPZ dynamics is to study the ratio between the spin current,  $j(r, t) = -\int_{-\infty}^r \partial_r q(r', t) dr'$ , and the polarization gradient. In rescaled diffusion, Fick’s law ensures that the two are proportional,  $j(r, t) \propto t^{1/3} \partial_r q(r, t)$ , while the nonlinearity of KPZ transport leads to the breakdown of this proportionality [16,23]. Crucially, as illustrated in Fig. 3(e), we find that the ratio is not constant (as would be predicted for rescaled diffusion) and rather is in good agreement with the KPZ prediction.

*Universality of KPZ dynamics.*—We now turn our attention to the conjecture that KPZ dynamics emerge in several broad classes of integrable models. We will focus on three distinct settings: (i) static models with generic non-Abelian symmetries, (ii) periodically driven (Floquet) models with non-Abelian symmetries, and (iii) supersymmetric models. In these latter two classes, even for the dynamical exponent, there are no generic results, although some particular instances are known to exhibit superdiffusion [23,48,72].

The construction of static, non-Abelian, integrable spin chains has a rich history, with different prescriptions for each of the four classes of simple Lie groups:  $\text{SU}(N)$ ,  $\text{SO}(2N)$ ,  $\text{SO}(2N+1)$ , and  $\text{SP}(2N)$  [25,39,60–66]. As detailed in the Supplementary Material, we construct nearest-neighbor models with the following four symmetries,  $\text{SU}(4)$ ,  $\text{SO}(3)$ ,  $\text{SO}(4)$  and  $\text{SP}(4)$ . Following our previous strategy for  $H_{\text{SU}(3)}$ , we analyze the transport dynamics of conserved charges for each of these models. In all cases, we observe excellent agreement with the KPZ universality class [Figs. 3(b) and 3(e)].

Extending this exploration to periodically driven systems requires systematically building the corresponding Floquet integrable models. Somewhat astonishingly, one can straightforwardly build such models from their static counterparts [36,73]. The Hamiltonian is divided into terms acting on even and odd bonds (denoted as  $H_{\text{even}}$  and  $H_{\text{odd}}$ , respectively), which are then alternately applied, leading to a Floquet unitary:  $U = e^{-iH_{\text{odd}}T/2} e^{-iH_{\text{even}}T/2}$ . Using this procedure, we can extend our analysis to the Floquet regime for all of the previous non-Abelian models [Figs. 3(c) and 3(e)]. Our conclusions are identical. The resulting transport falls within the KPZ universality class even though energy is no longer conserved.

Finally, let us consider integrable models where the non-Abelian symmetry is replaced with supersymmetry. Such models have been conjectured to exhibit superdiffusion, but observing this, either numerically or analytically, remains an open challenge [21,25]. Here, we focus on a pair of spinful fermionic lattice models: the  $t$ - $J$  model (with  $t = 2J$ ), and the Essler-Korepin-Schoutens (EKS) model [66,74–77]. These exhibit the two simplest supersymmetries,  $\text{SU}(1|2)$  and  $\text{SU}(2|2)$ , respectively.

The defining feature of models with supersymmetry is that their conserved charges fall into two types: bosonic and fermionic, although only the bosonic charge can in principle exhibit superdiffusion [21]. For the  $t$ - $J$  model, each lattice site can be occupied by either a spin-up fermion, a spin-down fermion, or a hole. The conserved bosonic charges are given by the total number of holes, and the total spin. Holes live in the Abelian U(1) sector and thus lack particle-hole symmetry leading to a finite Drude weight and ballistic transport [21]. Therefore, we study the spin polarization, given by the difference between the number of spin-up and spin-down particles. As before, we prepare a weak domain-wall in the spin polarization while keeping the other charge densities—including the hole density—constant.

For both the static and Floquet  $t$ - $J$  models, we observe superdiffusive spin transport (with  $z = 3/2$ ) via both the polarization transfer [Fig. 3(f)] and the collapse of the polarization profile [39]. The numerical evidence that spin transport falls within the KPZ universality class is more subtle. In particular, the polarization gradient,  $\partial_r q(r, t)$ , exhibits a discrepancy with both the KPZ and Gaussian expectations [Fig. 3(d)]. However, the finite-time flow of  $\partial_r q(r, t)$  approaches the KPZ scaling function in the same qualitative fashion as is observed in the SU(3) case [insets, Figs. 3(a) and 3(d)]; we conjecture that finite-time effects are exacerbated in supersymmetric models owing to the presence of additional ballistic modes [Fig. 3(g)] [78]. Moreover, a careful comparison of the relative error to the Gaussian model suggests that rescaled diffusion cannot be the correct limiting behavior [39].

*Experimental proposal.*—Recent advances in the control and manipulation of alkaline-earth atoms in optical lattices have opened the door to studying SU( $N$ )-symmetric spin models [79–88]. In particular, at unit filling in the Mott insulating phase, the lack of hyperfine coupling in the  $ns^2$   $^1S_0$  electronic ground state naturally leads to SU( $N$ )-symmetric spin-exchange interactions [87,89–91]:

$$H_{\text{SU}(N)} = J_{\text{SU}(N)} \sum_i \sum_{\alpha, \beta=1}^N \hat{s}_i^{\alpha, \beta} \hat{s}_{i+1}^{\beta, \alpha}, \quad (5)$$

where  $\hat{s}_i^{\alpha, \beta} = |\alpha\rangle\langle\beta|$  on site  $i$ ; in one dimension,  $H_{\text{SU}(N)}$  is integrable and precisely corresponds to the models considered above [e.g., Eq. (3)].

The observation and characterization of KPZ transport requires the ability to address two main experimental challenges: (i) preparing near infinite-temperature states with a well-defined domain-wall polarization and (ii) measuring the tails of the scaling function with sub-percent accuracy. The former can be accomplished via a two step process: first, optical pumping via an intercombination transition (e.g.,  $ns^2$   $^1S_0 \leftrightarrow nsnp$   $^3P_1$ ) can be used to generate arbitrary magnetization distributions which are preserved upon cooling to the Mott insulator [39]; second,

with single-site addressing [26,92–97], a coherent optical drive can be applied to half the system in order to prepare the domain wall.

Achieving the latter is significantly more subtle. In order to distinguish between KPZ dynamics and rescaled diffusion, careful estimates suggest the need to experimentally resolve the scaling function with a relative error of  $\sim 10^{-3}$  [39]. Achieving this error floor requires the ability to spatially resolve spin-transport dynamics over long time-scales and large distances. For concreteness, let us consider  $^{87}\text{Sr}$  atoms loaded into a two-dimensional optical lattice [87,98,99]. Recent experiments have demonstrated the elegant use of cavity enhancement to realize homogeneous lattices capable of supporting Mott insulators with a diameter of  $\sim 300$  sites [39,98]. By implementing strong confinement in one direction, one can subsequently divide the system into  $\sim 250$  independent chains, each with length  $\sim 150$  sites. Assuming an on-site interaction energy,  $U \sim 3$  kHz, and a tunneling rate,  $t \sim 300$  Hz, yields a spin-exchange interaction,  $J = 2t^2/U \approx 60$  Hz [39,98]. Optimizing for an evolution time of  $\sim 50/J$  and assuming an experimental cycle time of  $\sim 10$  s [87], we estimate that a relative error of  $\sim 10^{-3}$ , can be achieved within two days of averaging [39]. Finally, the presence of a finite density ( $\gtrsim 1\%$  [39,100]) of doublons and holes in the Mott insulator will perturb the polarization dynamics, but the exact nature of their effect remains an intriguing open question.

*Outlook.*—Since it was first observed in the spin-1/2 Heisenberg model [20], the microscopic origin of KPZ dynamics in integrable quantum magnets has remained a mystery [101]. Our Letter suggests that any such understanding will need to encompass a broader physical setting, including both Floquet and supersymmetric systems. In the context of supersymmetry, an intriguing direction is to characterize the impact of ballistic fermionic modes on the KPZ dynamics. Finally, the ability to experimentally measure the full counting statistics of spin transport opens the door to studying KPZ dynamics from a new perspective, which is currently challenging to access both analytically and numerically [26,102].

We gratefully acknowledge discussions with M. Aidelsburger, I. Bloch, V. Bulchandani, A. Kaufman, J. Moore, and J. Ye. We are especially indebted to S. Gopalakrishnan and R. Vasseur for introducing us to the framework of generalized hydrodynamics and for collaborations on related works. This work was supported by the U.S. Department of Energy, Office of Science, National Quantum Information Science Research Centers, Quantum Systems Accelerator (QSA), by the AFOSR MURI program (FA9550-21-1-0069), by the David and Lucile Packard foundation, and by the Alfred P. Sloan foundation. B. Y. acknowledges support from the US Department of Energy (BES Grant No. DE-SC0019241). F. M. acknowledges support from the Army Research Office (Grant

No. W911NF2110262). J. K. acknowledges support from the U.S. Department of Energy through the Quantum Information Science Enabled Discovery (QuantISED) for High Energy Physics (KA2401032) and through the GeoFlow Grant No. desc0019380.

\*These authors contributed equally to this work.

[1] M. Kardar, G. Parisi, and Y.-C. Zhang, *Phys. Rev. Lett.* **56**, 889 (1986).

[2] T. Halpin-Healy and Y.-C. Zhang, *Phys. Rep.* **254**, 215 (1995).

[3] I. Corwin, [arXiv:1106.1596](https://arxiv.org/abs/1106.1596).

[4] I. Corwin, [arXiv:1403.6877](https://arxiv.org/abs/1403.6877).

[5] J. Baik, P. Deift, and K. Johansson, *J. Am. Math. Soc.* **12**, 1119 (1999).

[6] P. Calabrese, P. Le Doussal, and A. Rosso, *Europhys. Lett.* **90**, 20002 (2010).

[7] V. Dotsenko, *Europhys. Lett.* **90**, 20003 (2010).

[8] G. Amir, I. Corwin, and J. Quastel, *Commun. Pure Appl. Math.* **64**, 466 (2011).

[9] V. Popkov, A. Schadschneider, J. Schmidt, and G. M. Schütz, *Proc. Natl. Acad. Sci. U.S.A.* **112**, 12645 (2015).

[10] I. Corwin, H. Shen, and L.-C. Tsai, in *Annales de l’Institut Henri Poincaré, Probabilités et Statistiques* (Institut Henri Poincaré, Berlin, 2018), Vol. 54 pp. 995–1012.

[11] K. Matetski, J. Quastel, and D. Remenik, *Acta Math.* **227**, 115 (2021).

[12] I. Corwin, N. O’Connell, T. Seppäläinen, and N. Zygouras, *Duke Math. J.* **163**, 513 (2014).

[13] J. de Gier, A. Schadschneider, J. Schmidt, and G. M. Schütz, *Phys. Rev. E* **100**, 052111 (2019).

[14] I. Corwin, P. Ghosal, H. Shen, and L.-C. Tsai, *Commun. Math. Phys.* **375**, 1945 (2020).

[15] L. Bertini and N. Cancrini, *J. Stat. Phys.* **78**, 1377 (1995).

[16] M. Prähofer and H. Spohn, *J. Stat. Phys.* **115**, 255 (2004).

[17] M. Hairer, *Ann. Math.* **178**, 559 (2013).

[18] T. Sasamoto and H. Spohn, *Nucl. Phys. B* **834**, 523 (2010).

[19] I. Corwin, [arXiv:1804.05721](https://arxiv.org/abs/1804.05721).

[20] M. Ljubotina, M. Žnidarič, and T. Prosen, *Nat. Commun.* **8**, 16117 (2017).

[21] E. Ilievski, J. De Nardis, M. Medenjak, and T. Prosen, *Phys. Rev. Lett.* **121**, 230602 (2018).

[22] S. Gopalakrishnan and R. Vasseur, *Phys. Rev. Lett.* **122**, 127202 (2019).

[23] M. Ljubotina, M. Žnidarič, and T. Prosen, *Phys. Rev. Lett.* **122**, 210602 (2019).

[24] A. Rubio-Abadal, J.-y. Choi, J. Zeiher, S. Hollerith, J. Rui, I. Bloch, and C. Gross, *Phys. Rev. X* **9**, 041014 (2019).

[25] E. Ilievski, J. De Nardis, S. Gopalakrishnan, R. Vasseur, and B. Ware, *Phys. Rev. X* **11**, 031023 (2021).

[26] D. Wei, A. Rubio-Abadal, B. Ye, F. Machado, J. Kemp, K. Srakaew, S. Hollerith, J. Rui, S. Gopalakrishnan, N. Y. Yao, I. Bloch, and J. Zeiher, *Science* **376**, 716 (2022).

[27] A. Scheie, N. Sherman, M. Dupont, S. Nagler, M. Stone, G. Granroth, J. Moore, and D. Tenant, *Nat. Phys.* **17**, 726 (2021).

[28] Ž. Krajnik, E. Ilievski, and T. Prosen, *SciPost Phys.* **9**, 038 (2020).

[29] Ž. Krajnik, E. Ilievski, and T. Prosen, *Phys. Rev. Lett.* **128**, 090604 (2022).

[30] S. Jeon and L. G. Yaffe, *Phys. Rev. D* **53**, 5799 (1996).

[31] A. G. Abanov, in *Applications of Random Matrices in Physics*, NATO Science Series II: Mathematics, Physics and Chemistry, edited by É. Brézin, V. Kazakov, D. Serban, P. Wiegmann, and A. Zabrodin (Springer Netherlands, Dordrecht, 2006), pp. 139–161.

[32] E. Bettelheim, A. G. Abanov, and P. Wiegmann, *Phys. Rev. Lett.* **97**, 246401 (2006).

[33] M. Blake, H. Lee, and H. Liu, *J. High Energy Phys.* **10** (2018) 127.

[34] C. D. White, M. Zaletel, R. S. K. Mong, and G. Refael, *Phys. Rev. B* **97**, 035127 (2018).

[35] B. Ye, F. Machado, C. D. White, R. S. K. Mong, and N. Y. Yao, *Phys. Rev. Lett.* **125**, 030601 (2020).

[36] M. Vanicat, L. Zadnik, and T. Prosen, *Phys. Rev. Lett.* **121**, 030606 (2018).

[37] J. De Nardis, D. Bernard, and B. Doyon, *SciPost Phys.* **6**, 049 (2019).

[38] We choose to work with open boundary conditions throughout this Letter. The boundary conditions do not affect the dynamics we observed within the timescale we considered [39]. However, a strict analytical approach may require a careful treatment of the boundary conditions, which is important and subtle in integrable systems [43,44].

[39] See Supplemental Material at <http://link.aps.org/supplemental/10.1103/PhysRevLett.129.230602> for a detailed check of accuracy of the numerical methods, details about the models studied, extra numerical results supporting the KPZ superdiffusion and other transport classes, and details about the proposed experimental realization. The Supplemental Material includes Refs. [40–42]; As detailed in the Supplemental Material, we construct nearest-neighbor models with the following four symmetries, SU(4), SO(3), SO(4), and SP(4) [63].

[40] U. Schollwöck, *Ann. Phys. (Amsterdam)* **326**, 96 (2011).

[41] W. J. Eckner, A. W. Young, N. Schine, and A. M. Kaufman, *Rev. Sci. Instrum.* **92**, 093001 (2021).

[42] J. De Nardis, S. Gopalakrishnan, R. Vasseur, and B. Ware, *Phys. Rev. Lett.* **127**, 057201 (2021).

[43] A. Gerrard and V. Regelskis, *Nucl. Phys. B* **952**, 114909 (2020).

[44] H. Frahm and M. J. Martins, *Nucl. Phys. B* **980**, 115799 (2022).

[45] G. Uimin, *Sov. J. Exp. Theor. Phys. Lett.* **12**, 225 (1970).

[46] C. Lai, *J. Math. Phys. (N.Y.)* **15**, 1675 (1974).

[47] B. Sutherland, *Phys. Rev. B* **12**, 3795 (1975).

[48] M. Dupont and J. E. Moore, *Phys. Rev. B* **101**, 121106(R) (2020).

[49] Here, we perturb  $H_{\text{SU}(3)}$  using SU(3)-symmetry-respecting, but integrability-breaking next-nearest-neighbor interactions. As expected for generic non-integrable models,  $\mathcal{P}(t) \sim t^{1/2}$ , consistent with diffusive transport [50–52].

[50] H. Spohn, *Large Scale Dynamics of Interacting Particles* (Springer Science & Business Media, 2012).

[51] B. Doyon, *J. Stat. Phys.* **186**, 25 (2022).

[52] A. J. Friedman, S. Gopalakrishnan, and R. Vasseur, *Phys. Rev. B* **101**, 180302(R) (2020).

[53] The agreement between DMT numerics and GHD analytics (which have different underlying assumptions) serves a dual benchmarking role; in particular, it highlights DMT's ability to faithfully characterize late-time transport dynamics and GHD's ability to quantitatively compute transport coefficients in integrable models [37,54].

[54] C. Karrasch, J. E. Moore, and F. Heidrich-Meisner, *Phys. Rev. B* **89**, 075139 (2014).

[55] J. De Nardis, S. Gopalakrishnan, E. Ilievski, and R. Vasseur, *Phys. Rev. Lett.* **125**, 070601 (2020).

[56] A. G. Izergin and V. E. Korepin, *Commun. Math. Phys.* **94**, 67 (1984).

[57] V. I. Vichirko and N. Y. Reshetikhin, *Theor. Math. Phys.* **56**, 805 (1983).

[58] K. Hao, J. Cao, G.-L. Li, W.-L. Yang, K. Shi, and Y. Wang, *J. High Energy Phys.* **06** (2014) 128.

[59] A. Izergin and V. Korepin, *Commun. Math. Phys.* **79**, 303 (1981).

[60] M. Jimbo, *Commun. Math. Phys.* **102**, 537 (1986).

[61] C. L. Schultz, *Phys. Rev. Lett.* **46**, 629 (1981).

[62] V. E. Korepin, N. M. Bogoliubov, and A. G. Izergin, *Quantum Inverse Scattering Method and Correlation Functions*, Cambridge Monographs on Mathematical Physics (Cambridge University Press, Cambridge, 1993).

[63] P. Kulish and E. Sklyanin, *J. Sov. Math.* **19**, 1596 (1982).

[64] P. Kulish, *J. Sov. Math.* **35**, 2648 (1986).

[65] C. Kassel, *Quantum Groups*, Graduate Texts in Mathematics (Springer-Verlag, New York, 1995).

[66] M. Martins and P. Ramos, *Nucl. Phys.* **B500**, 579 (1997).

[67] A systematic way to generate such integrable models with lower symmetries by breaking a non-Abelian symmetry is called q-deformation. The corresponding models models are often called q-deformed vertex models [60,61].

[68] P. Lévy and P. Lévy, *Théorie de l'addition des variables aléatoires* (Gauthier-Villars, Paris, 1954).

[69] M. F. Shlesinger, G. M. Zaslavsky, and U. Frisch, *Lévy Flights and Related Topics in Physics* (Springer, Berlin, 1995).

[70] M. K. Joshi, F. Kranzl, A. Schuckert, I. Lovas, C. Maier, R. Blatt, M. Knap, and C. F. Roos, *Science* **376**, 720 (2022).

[71] We use  $\partial_r$  as a short-hand for discrete difference in the our system:  $\partial_r q(r, t) = \langle \hat{q}_{r+1}(t) \rangle - \langle \hat{q}_r(t) \rangle$ .

[72] E. Ilievski, J. De Nardis, M. Medenjak, and T. Prosen, *Phys. Rev. Lett.* **121**, 230602 (2018).

[73] M. Ljubotina, L. Zadnik, and T. Prosen, *Phys. Rev. Lett.* **122**, 150605 (2019).

[74] S. Sarkar, *J. Phys. A* **24**, 1137 (1991).

[75] F. H. L. Essler, V. E. Korepin, and K. Schoutens, *Phys. Rev. Lett.* **68**, 2960 (1992).

[76] M. J. Martins, *Phys. Rev. Lett.* **74**, 3316 (1995).

[77] M. Martins, *Nucl. Phys.* **B450**, 768 (1995).

[78] Indeed, upon decreasing the hole density, we observe an improved convergence to KPZ universality. Note that when there are no holes, one recovers an SU(2)-symmetric model. Curiously, this suggests that KPZ dynamics might arise in supersymmetric systems for generic fermionic filling fractions.

[79] C. Weitenberg, M. Endres, J. F. Sherson, M. Cheneau, P. Schauß, T. Fukuhara, I. Bloch, and S. Kuhr, *Nature (London)* **471**, 319 (2011).

[80] G. Cappellini, M. Mancini, G. Pagano, P. Lombardi, L. Livi, M. Siciliani de Cumis, P. Cancio, M. Pizzocaro, D. Calonico, F. Levi, C. Sias, J. Catani, M. Inguscio, and L. Fallani, *Phys. Rev. Lett.* **113**, 120402 (2014).

[81] G. Pagano, M. Mancini, G. Cappellini, P. Lombardi, F. Schäfer, H. Hu, X.-J. Liu, J. Catani, C. Sias, M. Inguscio, and L. Fallani, *Phys. Rev. Lett.* **10**, 198.

[82] F. Scazza, C. Hofrichter, M. Höfer, P. C. De Groot, I. Bloch, and S. Fölling, *Nat. Phys.* **10**, 779 (2014).

[83] X. Zhang, M. Bishof, S. L. Bromley, C. V. Kraus, M. S. Safronova, P. Zoller, A. M. Rey, and J. Ye, *Science* **345**, 1467 (2014).

[84] M. Miranda, R. Inoue, Y. Okuyama, A. Nakamoto, and M. Kozuma, *Phys. Rev. A* **91**, 063414 (2015).

[85] R. Yamamoto, J. Kobayashi, T. Kuno, K. Kato, and Y. Takahashi, *New J. Phys.* **18**, 023016 (2016).

[86] M. Miranda, R. Inoue, N. Tambo, and M. Kozuma, *Phys. Rev. A* **96**, 043626 (2017).

[87] L. Sonderhouse, C. Sanner, R. B. Hutson, A. Goban, T. Bilitewski, L. Yan, W. R. Milner, A. M. Rey, and J. Ye, *Nat. Phys.* **16**, 1216 (2020).

[88] N. Schine, A. W. Young, W. J. Eckner, M. J. Martin, and A. M. Kaufman, [arXiv:2111.14653](https://arxiv.org/abs/2111.14653).

[89] A. V. Gorshkov, M. Hermele, V. Gurarie, C. Xu, P. S. Julienne, J. Ye, P. Zoller, E. Demler, M. D. Lukin, and A. M. Rey, *Nat. Phys.* **6**, 289 (2010).

[90] C. Hofrichter, L. Riegger, F. Scazza, M. Höfer, D. R. Fernandes, I. Bloch, and S. Fölling, *Phys. Rev. X* **6**, 021030 (2016).

[91] H. Ozawa, S. Taie, Y. Takasu, and Y. Takahashi, *Phys. Rev. Lett.* **121**, 225303 (2018).

[92] W. S. Bakr, A. Peng, M. E. Tai, R. Ma, J. Simon, J. I. Gillen, S. Fölling, L. Pollet, and M. Greiner, *Science* **329**, 547 (2010).

[93] J. F. Sherson, C. Weitenberg, M. Endres, M. Cheneau, I. Bloch, and S. Kuhr, *Nature (London)* **467**, 68 (2010).

[94] L. W. Cheuk, M. A. Nichols, M. Okan, T. Gersdorf, V. V. Ramasesh, W. S. Bakr, T. Lompe, and M. W. Zwierlein, *Phys. Rev. Lett.* **114**, 193001 (2015).

[95] M. F. Parsons, F. Huber, A. Mazurenko, C. S. Chiu, W. Setiawan, K. Wooley-Brown, S. Blatt, and M. Greiner, *Phys. Rev. Lett.* **114**, 213002 (2015).

[96] A. Omran, M. Boll, T. A. Hilker, K. Kleinlein, G. Salomon, I. Bloch, and C. Gross, *Phys. Rev. Lett.* **115**, 263001 (2015).

[97] E. Haller, J. Hudson, A. Kelly, D. A. Cotta, B. Peaudecerf, G. D. Bruce, and S. Kuhr, *Nat. Phys.* **11**, 738 (2015).

[98] A. J. Park, J. Trautmann, N. Šantić, V. Klüsener, A. Heinz, I. Bloch, and S. Blatt, [arXiv:2110.08073](https://arxiv.org/abs/2110.08073).

[99] T. Bothwell, C. J. Kennedy, A. Aeppli, D. Kedar, J. M. Robinson, E. Oelker, A. Staron, and J. Ye, *Nature (London)* **602**, 420 (2022).

[100] E. Ibarra-García-Padilla, S. Dasgupta, H.-T. Wei, S. Taie, Y. Takahashi, R. T. Scalettar, and K. R. A. Hazzard, *Phys. Rev. A* **104**, 043316 (2021).

[101] V. B. Bulchandani, *Phys. Rev. B* **101**, 041411(R) (2020), publisher: American Physical Society.

[102] S. Gopalakrishnan, A. Morningstar, R. Vasseur, and V. Khemani, [arXiv:2203.09526](https://arxiv.org/abs/2203.09526).